Published in final edited form as:
Mol Microbiol. 2012 April ; 84(1): 181–197. doi:10.1111/j.1365-2958.2012.08018.x.

Cardiolipin synthase is required for *Streptomyces coelicolor* morphogenesis

Vinod Jyothikumar[1], **Khanungkan Klanbut**[1], **John Tiong**[1], **James S. Roxburgh**[1], **Iain S. Hunter**[1], **Terry K. Smith**[2], and **Paul R. Herron**[1,*]

[1]Strathclyde Institute of Pharmacy and Biomedical Sciences, University of Strathclyde, 161 Cathedral Street, Glasgow G4 0RE, UK.

[2]Biomolecular Sciences Research Complex, University of St Andrews, North Haugh, St Andrews, Fife KY16 9ST, UK.

Summary

The fluid mosaic model has recently been amended to account for the existence of membrane domains enriched in certain phospholipids. In rod-shaped bacteria, the anionic phospholipid cardiolipin is enriched at the cell poles but its role in the morphogenesis of the filamentous bacterium *Streptomyces coelicolor* is unknown. It was impossible to delete *clsA* (cardiolipin synthase; *SCO1389*) unless complemented by a second copy of *clsA* elsewhere in the chromosome. When placed under the control of an inducible promoter, *clsA* expression, phospholipid profile and morphogenesis became inducer dependent. TLC analysis of phospholipid showed altered profiles upon depletion of *clsA* expression. Analysis of cardiolipin by mass spectrometry showed two distinct cardiolipin envelopes that reflected differences in acyl chain length; the level of the larger cardiolipin envelope was reduced in concert with *clsA* expression. ClsA-EGFP did not localize to specific locations, but cardiolipin itself showed enrichment at hyphal tips, branch points and anucleate regions. Quantitative analysis of hyphal dimensions showed that the mycelial architecture and the erection of aerial hyphae were affected by the expression of *clsA*. Overexpression of *clsA* resulted in weakened hyphal tips, misshaped aerial hyphae and anucleate spores and demonstrates that cardiolipin synthesis is a requirement for morphogenesis in *Streptomyces*.

Introduction

The original fluid-mosaic model of membrane structure and function (Singer and Nicolson, 1972) proposed that the cell membrane is comprised of a homogenous and free-moving assembly of phospholipids (PLs). More recently it has become clear that in eukaryotes, cholesterol-derived lipid rafts are involved in shaping the cell. To date, cholesterol biosynthesis has not been found in prokaryotes, but mathematically derived predictions indicate that, if a membrane PL has a large intrinsic curvature, PLs will form clusters large enough to localize to regions of negative curvature within the cell (Huang *et al.*, 2006; Renner and Weibel, 2011). Membrane components with a high degree of curvature include the anionic PL, cardiolipin (CL), which is found in the membranes of bacteria and mitochondrial cristae (Mileykovskaya and Dowhan, 2009). CL or diphosphatidylglycerol

*For correspondence. paul.herron@strath.ac.uk; Tel. (+44) 141 5482531; Fax (+44) 141 5484124..

Supporting information Additional supporting information may be found in the online version of this article.

Europe PMC Funders Author Manuscripts

consists of two phosphatidyl moieties joined by a glycerol and, as such, possesses four hydrophobic acyl chains and a small hydrophilic head group. It is this conical structure that allows CL to accumulate in membrane domains of higher curvature. Visualization of CL-rich membrane domains is carried out using 10-*N*-nonyl acridine orange (NAO), a fluorescent dye that has a higher affinity for CL than other anionic PLs. Upon aggregation with CL, NAO undergoes a green to red shift in its fluorescence emission maximum (Mileykovskaya and Dowhan, 2009). This dye was used to localize CL in both Gram-positive and Gram-negative bacteria (Mileykovskaya and Dowhan, 2005; Matsumoto *et al.*, 2006). For example, in *Escherichia coli*, CLis found at septal and polar regions of the cell (Mileykovskaya and Dowhan, 2000). Similarly, in the spore-forming bacterium *Bacillus subtilis* CL is also found at septal and polar sites, as well as on the fore-spore membrane (Kawai *et al.*, 2004). CL is also implicated in the localization of proteins to the cell poles such as ProP in *E. coli* (Romantsov *et al.*, 2007) where it contributes to the osmotic stress response (Romantsov *et al.*, 2008). In *B. subtilis*, phosphatidylglycerol (PG), the immediate precursor of CL, is involved in the recruitment of the cell division protein MinD to the cell membrane (Barak *et al.*, 2008). As a result, it is becoming increasingly apparent that anionic PLs and CL in particular, may play a role in directing bacterial proteins to the correct cellular location. Despite localization of CL-enriched domains in other bacteria, patterns of CL distribution in filamentous bacteria such as *Streptomyces* remains unknown. In *Streptomyces* little is known about the spatial heterogeneity of PLs within cell membranes, although compositional analysis of *Streptomyces hygroscopicus* showed that CL and lyso-CL make up around 25% of PLs (Hoischen *et al.*, 1997). *Streptomyces pristinaespiralis* contains much higher levels of CL, up to 65% (Limonet *et al.*, 2007), while the related organism, *Mycobacterium tuberculosis*, contains around 30% CL (Jackson *et al.*, 2000). Using the membrane-specific stain, FM4-64, on submerged cultures of *Streptomyces coelicolor*, some zones of mycelium stained more intensely than others, presumably due to the presence of membrane domains with greater affinity for the dye (Manteca *et al.*, 2008). Following the construction of a genome scale metabolic network of the model streptomycete, *S. coelicolor* (Borodina *et al.*, 2005), *SCO1389* (*clsA*) was predicted to encode a CL synthase that operates by a eukaryotic mechanism through the condensation of PG with CDP-diacylglycerol to form CL and CMP as opposed to the condensation of two PG molecules to form CL and glycerol that is found in other prokaryotes (Schlame *et al.*, 2000). Using an *in vitro* assay, this prediction was confirmed when ClsA was shown to catalyse the condensation of CDP-diacylglycerol and PG to form CL and *clsA* was able to restore CL synthesis in a CL-deficient strain of *Rhizobium etli* (Sandoval-Calderon *et al.*, 2009).

To determine if CL plays a role in streptomycete growth and morphogenesis we set out to delete *SCO1389* (*clsA*) from the *S. coelicolor* chromosome, investigate the existence and location of CL-enriched domains in *S. coelicolor* and determine the consequences of modulating levels of CL within a streptomycete mycelium.

Results

clsA is an essential gene in *S. coelicolor*

Bioinformatic analysis suggested that *clsA* encodes a putative CL synthase that operates with a eukaryotic mechanism (Borodina *et al.*, 2005). This was subsequently confirmed by a biochemical approach (Sandoval-Calderon *et al.*, 2009). We took a genetic approach to investigate the function of *clsA* in *S. coelicolor* M145 and attempted to disrupt this gene by Tn*5062* semi-targeted *in vitro* transposon mutagenesis (see *Experimental procedures*) (Bishop *et al.*, 2004; Herron *et al.*, 2004; Fernandez-Martinez *et al.*, 2011). The selection for a Tn*5062* insertion in *clsA* only gave rise to apramycin-resistant (am^r) kanamycin-resistant (km^r) colonies via a single recombination event and thus retained an intact copy of *clsA*.

When we attempted to generate a *clsA* null mutant by PCR-targeted mutagenesis (see *Experimental procedures*) (Gust *et al.*, 2003), despite screening over 1000 colonies for the am^r km^s phenotype indicative of an allelic replacement of *clsA* with Δ*clsA::am*^{r} (Fig. 1), all colonies displayed the am^r km^r phenotype indicative of a single recombination event (one of these colonies was designated RJ111, see below). The failure to obtain am^r km^s colonies suggests either that allelic exchange could not occur easily or that *clsA* is an essential gene. In order to test if *clsA* could be deleted in the presence of a second copy of *clsA* we introduced a complementing plasmid, pCLS105 (Table 1) into RJ111. Analysis of the resulting transconjugant colonies showed that 10% had the am^r, km^s, hyg^r phenotype that was indicative of deletion of the native *clsA* allele and replacement with Δ*clsA::am*^{r} via a double recombination event (Fig. 1). Southern analysis (data not shown) confirmed that these transconjugants, one of which was termed RJ114, had undergone a deletion of the parental copy of *clsA*, but carried a second copy of this gene integrated at $attB_{\Phi BT1}$ (Fig. 1). As we were only able to delete *clsA* when the gene product was provided by a second functional copy of *clsA* elsewhere in the chromosome, we concluded that *clsA* is an essential gene. To further test the requirement of *clsA* for viability, we constructed pAV117B1 (Table 1) that contained *clsA* under the control of the tetracycline-inducible *tetris* cassette (Rodriguez-Garcia *et al.*, 2005). When this plasmid was transferred via conjugation to RJ111, it was only possible to isolate colonies that had undergone deletion of the parental copy of *clsA* when the agar was supplemented with the cassette's inducer, anhydrotetracycline (atc). This strain, RJ118b, was also confirmed to have undergone a deletion of the parental copy of *clsA* by Southern analysis (data not shown) and was used to investigate the function of *clsA* by partial depletion. Surprisingly, RJ118b was able to grow weakly in the absence of atc; despite the fact that RJ118b could only be isolated from conjugation plates supplemented with atc. Subsequent analysis showed that the *tcp830* promoter was active even in the absence of atc (see below). Inducer-dependence of *clsA* expression in RJ118b for growth was determined by streaking spores of this strain along a concentration gradient of atc (0–1.5 μg ml^{-1} atc) on 3MA. RJ118b was only able to develop normally at concentrations of atc above a certain threshold level that we estimate to be around 5 ng ml^{-1} atc (Fig. 2A). RJ118b could grow vegetatively in the absence of inducer and indeed was able to display weak development after prolonged incubation (data not shown) and suggested that there was some leaky expression from the *tcp830* promoter even in the absence of atc. To confirm the atc dependence of *tcp830-clsA* expression, we isolated RNA from 48 h 3MA-grown cultures of M145 and RJ118b supplemented with different concentrations of atc and carried out semi-quantitative PCR (Fig. 2B). Increasing levels of atc resulted in increased expression of *tcp830-clsA* and demonstrated atc-dependent *clsA* expression, while *clsA* expression in M145 was unaffected by atc concentration. An RT-PCR product from *clsA* was seen in the absence of atc that is consistent with the growth of RJ118b without inducer; although it is unclear why we were unable to isolate *am*^{r} *km*^{s} *hyg*^{r} transconjugants of RJ111 and pAV117B1 in the absence of atc. The *tcp830* promoter displays weak uninduced activity in *S. coelicolor* when used in supplemented minimal medium (Rodriguez-Garcia *et al.*, 2005) and we believe that it is this low activity that accounts for the weak growth of RJ118b substrate hyphae, but is insufficient to permit normal development. Analysis of PLs from these cultures by thin-layer chromatography (TLC) demonstrated a change in PL profile brought about by the addition of atc to RJ118b (Fig. 2C, compare 0 ng ml^{-1} atc with 7.5 ng ml^{-1} and higher), while the PL profile of M145 was not significantly affected by atc. A PL spot that corresponded to the CL marker was absent from the profile of RJ118b grown without atc.

ClsA depletion alters the PL profile of *S. coelicolor*

To further analyse the PL profile of *S. coelicolor*, we investigated PLs produced by *S. coelicolor* during *clsA* depletion and overexpression following extraction from mid-log

phase liquid cultures. PLs from *S. coelicolor* M145, RJ117 (vector only control), RJ118b and RJ110 (*clsA* under the control of the thiostrepton-inducible *tipA* promoter) in the presence and absence of atc or thiostrepton were extracted from mycelial pellets and visualized by TLC (Fig. 3A). Liquid-grown RJ118b, grown without atc, displayed a slightly different TLC pattern to solid-grown cultures (see Fig. 2C, RJ118b, 0 ng ml^{-1} atc), but still showed reduced production of one or more PLs (Fig. 3A, spot A) and increased production of another PL (Fig. 3A, spot B) when compared with *S. coelicolor* M145 that approximately corresponded to the CL and PG markers respectively. The addition of atc restored the PL profile of RJ118b to that of the wild-type strain. Overexpression of *clsA* was carried out in RJ110, where, even in the absence of inducer, the *tipA* promoter is relatively strong (Ali *et al.*, 2002). It is unsurprising therefore that RJ110 grown in the absence of thiostrepton showed a similar TLC pattern to M145. However upon addition of thiostrepton, the PL (Fig. 3A, spot C) corresponding to CL showed a marked increase in intensity that is consistent with the predicted effect of *clsA* overexpression (Sandoval-Calderon *et al.*, 2009). Surprisingly, overexpression of *clsA* also displayed an increase of a spot (Fig. 3A, spot D) that corresponded to the PG marker.

ClsA depletion produces new PL species in *S. coelicolor*

In order to analyse the precursors of CL in more detail, we carried out electrospray mass spectrometry (MS) in negative ion mode by survey scans between 600 and 1000 m/z of PL extracts from mid-log phase liquid-grown cultures (Fig. S1). The PL profiles of the strains showed several differences in the various envelopes of peaks corresponding to phosphatidic acid (PA) (600–680 and 790–840 m/z), phosphatidylethanolamine (PE) (650–700 m/z), phosphatidylglycerol (PG) (700–750 and 850–890 m/z) and phosphatidylinositol (PI) (780–840 m/z) species. A full lipidomic analysis of *S. coelicolor* will be published elsewhere (T.K. Smith and P.R. Herron, in preparation). RJ118b, grown without atc (Fig. S1B), showed a reduction in several PA species (Sud *et al.*, 2007) between 600 and 660 m/z when compared with M145 (Fig. S1A) and when RJ118b was grown with atc (Fig. S1C). RJ118b, grown without atc, also showed an increase in PG species of m/z between 700 and 750 that have a lower relative abundance in M145 (Fig. S1A) or RJ118b grown with atc (Fig. S1C). The identity of these species as PA or PG was confirmed following fragmentation analysis of CL (see below) (Sud *et al.*, 2007). The changes in PA and PG content are consistent with a reduction in CL synthesis leading to an increase of these precursors of CL (Sandoval-Calderon *et al.*, 2009).

Mass spectrometric analysis was also carried out to investigate the effect of ClsA depletion on CL in *S. coelicolor* in greater detail. PL extracts of mid-log-phase liquid-grown cultures of M145 and RJ118b were analysed by electrospray MS in negative ion mode, by either survey scans between 1000 and 2000 m/z or collision-induced fragmentation of parents of 153 m/z at collision energy of ~ 70 V. Survey scans in the 1000–2000 m/z allow detection of large PLs such as CL and analysis of M145 showed two envelopes of CL species (Fig. 3B, panel 1). The main species in the two envelopes of CL lay between 1308 and 1390 m/z, and between 1458 and 1528 m/z, which corresponded to CL containing total fatty acids equivalent to C60:0 to C67:5 and C71:0 to C77:5 (total number of carbons:total number of double bonds) respectively. The molecular ions either side of 1348 m/z are CL species that differ by one methylene group and a number of double bonds, demonstrating the heterogeneity of the fatty acids present in these CL species. Daughter ion spectra of CL species from 1348 and 1500 m/z were conducted (Figs S2 and S3) and showed that they are very heterogeneous. For example the species at 1348 m/z contains various molecular species consisting of PA moieties containing C14 to C17 fatty acids with none, one or two double bonds. The second envelope of M145 CL species (Fig. 3B, panel 2), including the molecular species at 1500 m/z, also contained C14 to C17 fatty acids with none, one or two double

bonds. However, this high-mass collection of CL species also contained a PA moiety that had fatty acids significantly higher than C17 centred on the peak at 809.2 (Fig. S3A) and is further demonstrated by the lyso-PA and lyso-PA-1,2-cyclic phosphate ions at 571, 552.8 m/z respectively (Fig. S3). The predicted fragmentation pathway (Fig. S3B) indicates that this fatty acid moiety at the sn-1 position should have a mass of 416 m/z, which, if a straight chain fatty acid, would have to be C28:4 (Sud *et al.*, 2007). Although we were able to detect the parents of this species at 809.2 and 571 m/z, we were unable to observe the 416 m/z fatty acid species (Fig. S3A). It is likely that our failure to detect this species was due to a general phenomenon where longer chain fatty acids become harder to ionize due to an increase in the mass to charge and are often difficult to detect.

Collectively, these two distinct pools of CL species probably gave rise to a heterogeneous CL TLC spot (Fig. 3A), as compared with the CL standard, which is primarily one species containing four C18:2 fatty acids (Fig. 3A, lane M) (Morita and Englund, 2001). RJ118b, grown without atc, showed a different profile of CL species compared with M145 (Fig. 3B, panel 2). The lower-molecular-weight CL species (1296–1363 m/z) were still present; however, the higher-molecular-weight CL species (1458–1527 m/z) were significantly reduced, almost absent. The spectra also revealed a new collection of related ions at a lower molecular weight (1070–1137 m/z), these were identified as mono-lyso CL species of those CL species present at 1296–1363 m/z. These changes in the CL species were reflected by the changes in the PL species observed by TLC (Fig. 3A, RJ118b no atc); first the CL spot is less intense and second there is now a more intense spot (B) with an approximate Rf corresponding to the PG standard (primarily C34). It is likely that this spot, which is more intense than M145, corresponds to the relative increase in the PG (C30-34) as demonstrated by the relative increase of PG species shown in Fig. S1 brought about by the lack of formation of the higher-molecular-weight CL species (1458–1528 m/z, C71:0 to C77:5) (Sandoval-Calderon *et al.*, 2009).

RJ118b, grown with atc (Fig. 3B, panel 3), did not display a full restoration of the wild-type CL profile. The unmodified CL species (1296–1363 m/z), as well as species at ~ 1500 m/z (low abundance), similar to those seen with M145 (Fig. 3B, panel 1) were observed. However, as well as these CL species, a new intense envelope of CL species (~ 1200–1300 m/z) was observed upon induction with atc (Fig. 3B, compare panels 2 and 3). These new CL species (~ 1200–1300 m/z) were similar to those observed at 1296–1363 m/z, except that they had a higher percentage of short-chain fatty acids (C14:0–C17:0) following fragmentation analysis (Fig. S4). For example, following fragmentation of the heterogeneous 1256.6 m/z species, it was possible to identify the presence of PA with a C17 and a C14 fatty acid, shown by the fragment ions of PA at 633 (C31) and lyso-PA at 381 m/z (C14) respectively. This demonstrates that this envelope of CL species contain total fatty acids equivalent to C55:0 to C60:0. In addition the PG spot (C30–34) observed when RJ118b was grown without atc, decreased when grown with atc (Fig. 3A), as these lipid moieties are being used to form the new CL species. The faint presence of CL in RJ118b grown in the absence of inducer provides further evidence for the leaky activity of the *tcp830* promoter.

Overexpression of *clsA* results in altered morphology of substrate, aerial hyphae and spores

pCLS113A (Table 1), which contains *clsA* fused to the *tipA* promoter, was integrated into the phage attachment site, $attB_{\Phi C31}$ of M145 via conjugation. Following confirmation by Southern blotting and restriction analysis (data not shown), a transconjugant, RJ110, was selected for further investigation. The effect of altering expression of *clsA* on streptomycete growth and branching was studied by growing M145, RJ118b, VJ8600 and RJ110 on 3MAin the presence and absence of atc or thiostrepton while measuring a number of

parameters that describe mycelial architecture quantitatively (Fig. 4) from still images. These data, in a tabulated form, are provided in Table S1. Statistical analysis of treated and untreated samples was carried out with the Student's *t*-test between treated (with atc or thiostrepton) and untreated strains, the results of which are provided in Table S2. Increasing expression of *clsA*, brought about by the addition of either atc or thiostrepton, led to an increase in hyphal width (1) from 0.51 (± 0.01) μm to 0.67 (± 0.16) μm and 1.21 (± 0.26) μm respectively. This increase in diameter was also found in aerial hyphae and spores where the highest levels of induction by thiostrepton lead to an increase in spore width (2) from 0.96 (± 0.02) μm in uninduced M145 to 1.89 (± 0.40) μm. Alteration of expression levels of *clsA* also reduced the distance with which growing *S. coelicolor* hyphae grew before changing direction (3); depletion of *clsA* lead to an increase in this distance from 2.99 (± 0.68) μm to 4.90 (± 0.79) μm, while overexpression with thiostrepton lead to a reduction in this distance to 1.98 (± 0.23) μm. This effect was also apparent in the angle through which the extending hypha bent when changing direction (5); uninduced wild-type *S. coelicolor*, bent at an angle of 142° (± 2.75°) when changing direction (no change in direction would be 180°), while depletion and overexpression of *clsA* altered this angle to 157° (± 5.2°) and 102° (± 19.5°) respectively. Branching was also affected by levels of *clsA* expression; depletion increased the average inter-branch distance (4) from 6.23 (± 1.63) μm to 13.88 (± 4.97) μm, while overexpression decreased the inter-branch distance to 2.75 (± 1.00) μm. Similarly branching angle was also affected, although both depletion and overexpression of *clsA* led to a decrease in branching angle (6) to 101° (± 3.95°) and 82° (± 8.80°) respectively from 112° (± 5.69°) in the uninduced wild-type strain. Taken together these data suggest that if *clsA* expression was depleted, and consequently CL levels reduced, *S. coelicolor* hyphae changed direction and branched less often. In contrast when *clsA* was overexpressed hyphae changed direction and branched more frequently.

As alteration of *clsA* expression levels changed hyphal width and the frequency with which growing substrate hyphae changed direction we speculated that this might be due to an altered PL content of membrane regions positioned at the hyphal tip. As such, growing hyphal tips might behave in an unusual fashion when observed by time-lapse microscopy. This was investigated by generating movies of RJ110 grown in the presence of thiostrepton. Overexpression of *clsA* resulted in two phenotypes. First, hyphal tips frequently underwent a division into two daughter hyphae (Fig. 5A) rather than through a branch point appearing some distance from the hyphal tip (Jyothikumar *et al.*, 2008). Second, hyphal tips were often observed to undergo spontaneous lysis (Fig. 5B). We have not previously seen splitting or spontaneous lysis of hyphal tips while viewing of movies of other *S. coelicolor* strains, suggesting that overexpression of *clsA* leads to a weakening of the tip integrity, presumably through an alteration of PL content at the tip. Both movies are available as supplementary files (Fig. S4A and B).

As adequate *clsA* expression was required for normal development it was difficult to investigate the effect of depletion of *clsA* on spore morphology. However by adding thiostrepton to 3MA-grown coverslip cultures of *S. coelicolor* RJ110 (*clsA* under the control of the strong *tipA* promoter, Table 1), it was possible to examine the effect of overexpressing *clsA*. Nucleoids, sites of peptidoglycan incorporation and membranes were visualized using Syto42, Vancomycin-FL and FM4-64 respectively in live cells of VJ8600 (Fig. 6A) and RJ110 (Fig. 6B). Aerial hyphae of RJ110, grown in the presence of thiostrepton were aberrant, often branched and showed region of PL enrichment demonstrated via bright FM4-64 foci; these regions often coincided with regions of Vancomycin-FL staining although it is not possible to say whether CL is responsible for branch initiation or that it accumulates at branch sites. Spores of RJ110, grown under the same conditions were rare, but large and aberrant, and were often anucleate (Fig. 6C), indicating that CL plays a role in nucleoid localization during hyphal development.

CL, but not ClsA, localizes to hyphal tips and branch points

To determine the cellular location of ClsA, pCLS108B (Table 1) (which contains *clsA* fused, in-frame, to *egfp*) was integrated into $attB_{\Phi BT1}$ of RJ111 by conjugation in an analogous procedure to the creation of RJ114 (Fig. 1). Hyg^r am^r km^s transconjugants were isolated that had lost the parental copy of *clsA* by a second recombination event; the null mutation being complemented by *clsA-egfp*. One of these transconjugants was termed RJ113 and was confirmed through Southern blotting and restriction analysis (data not shown). When grown on 3MA, a background of faint fluorescence was often seen in vegetative hyphae of M145 and exposure conditions were adjusted so that this auto fluorescence was invisible. RJ113 showed strong fluorescence mostly in the substrate hyphae and in young aerial hyphae (Fig. 7A). Faint punctate signals were occasionally observed at the base of mature RJ113 aerial hyphae, but such signals were weak and inconsistent in comparison with the strong fluorescence in substrate hyphae. When M145 and atcinduced RJ118b were stained with NAO (Fig. 8), both showed staining at hyphal tips (93% and 88% respectively) and branch points and (89% and 98% respectively). The dependence of tip and branch point staining on *clsA* expression was demonstrated by the fact that, without atc, 12% of RJ118b tips and 8% of branch points stained with NAO. This dye stains all anionic PLs green and CL red when excited with blue or green light respectively (Mileykovskaya and Dowhan, 2009); fluorescent regions demonstrated both forms of fluorescence indicating that the anionic PL visualized was indeed CL. It was also apparent that regions to which NAO localized did not also stain with Syto42, indicating that nucleoids were absent from regions rich in anionic PLs.

Discussion

Although streptomycetes grow by hyphal extension, little is known about the mechanisms by which these processes are directed (Flardh, 2003b). For apical extension to occur, new cell wall material and, presumably, membrane PLs are deposited at the tip rather than along the lateral walls of an extending hypha (Daniel and Errington, 2003). Consequently the hyphal tip must possess some unique properties that mark it as a site for extension. The fact that hyphal tips and branches show regions enriched in anionic PLs and CL (Fig. 8) suggest that sites of CL enrichment may be a means to label regions as sites for the incorporation of new cellular material. CL is found at regions of membrane-negative curvature (Renner and Weibel, 2011) such as the polar regions of *E. coli* and *B. subtilis* (Mileykovskaya and Dowhan, 2005; Matsumoto *et al.*, 2006), so it is perhaps unsurprising that it is also found at the *Streptomyces* hyphal tip, which is similar to the pole of unicellular bacteria in terms of negative curvature. The retarded growth of RJ118b in the absence of inducer indicates that some expression of the gene occurs under these conditions and was confirmed by RT-PCR and PL analysis by TLC. When the *tcp830* promoter was used to drive expression of bacterial luciferase, some activity was detected in the absence of inducer which suggests that the promoter is leaky to some degree (Rodriguez-Garcia *et al.*, 2005).

Depletion of atc from RJ118b caused significant changes in the PL TLC profiles when compared with wild-type *S. coelicolor* while addition of inducer to RJ118b restored the wild-type PL profile *S. coelicolor*. Despite it not being possible to conclusively identify all the PLs by TLC, in conjunction with MS analysis, most of the differences that relate to CL synthesis between the strains can be explained. Comparison of the observed spots with the Rfs of several PL standards and similar analyses in the literature (Hoischen *et al.*, 1997; Sandoval-Calderon *et al.*, 2009) indicate that depletion of *clsA* caused a decrease in intensity of CL and a corresponding increase in the intensity of the spots that correspond to PG. This is consistent with ClsA synthesizing CL from PG and CDP-DAG (Sandoval-Calderon *et al.*, 2009).

Analysis of CL by mass spectrometry highlighted the complexity of streptomycete PLs and a full lipidomic analysis of the PL species in *S. coelicolor* will be published in due course (T.K. Smith and P.R. Herron, in preparation). Wild-type *S. coelicolor* contained two envelopes of CL between 1308 and 1390 m/z and between 1458 and 1528 m/z, corresponding to CLs containing total fatty acids equivalent to C60:0 to C67:5 and C71:0 to C77:5 respectively. Although addition of inducer to RJ118b did not restore the wild-type CL pattern (Fig. 3B), when this strain was grown without atc the larger 1458–1528 m/z envelope disappeared. In addition, depletion of ClsA when RJ118b was grown without atc generated additional peaks corresponding to PA following MS analysis (Sud *et al.*, 2007) and an increase in the PG (C30–C34) species when compared with the wild-type strain (Fig. S2B and A respectively). The relative changes in PA and PG with C14–C17 fatty acids during ClsA depletion is understandable, as a reduction in CL synthesis (the CL fragmentation analysis in Figs S2B, S3B and S4B clearly shows PA ions with C14–C17 fatty acids), would lead to an increase in the corresponding precursors. However, it is worth noting that the PA species that correspond to the higher-mass fragments (795, 809, 823, 837 m/z) (850–890 m/z) that would be associated with the larger (1458–1528 m/z) CL species (Fig. S2B), did not show a relative increase when comparing RJ118b grown without atc (Fig. S1B) and M145 (Fig. S1A) and neither do the corresponding PG species (850–890 m/z). This shows that the PA and PG species that should contain the extra long fatty acid did not increase as they did for the shorter chain PA and PG following ClsA depletion. This may be due to a limiting amount of extra long fatty acid at a specific location, or the larger CLs are made *in situ* via remodelling by formation of mono-lyso-CL by a specific acyl-transferase. This also might explain why that, with addition of atc to RJ118b, only lyso-CL was formed; proper regulation of *clsA* expression and/or access to the correct substrates might ultimately be determined by the available fatty acids and/or the availability of further processing enzyme activities.

RJ118b, when grown in the absence of atc, was only able to erect aerial hyphae after prolonged incubation, showing that CL, either directly or indirectly, was necessary for the aerial hyphae to break the surface tension of the air–water interface. When RJ118b was plated next to M145 in the absence of atc, no development was observed along the RJ118b colony edge closest to that of M145 (data not shown) and demonstrates that ClsA or CL do not form part of the developmental signalling cascade into which many *S. coelicolor bld* mutants can be placed (Nodwell *et al.*, 1996). However, while it is not possible to exclude that CL is directly responsible for allowing aerial hyphae to break the surface tension of the air–water interface, it is possible that CL acts in an indirect fashion through interaction with other cellular components required for development at the base of aerial hyphae (Willey *et al.*, 2006).

Alteration in levels of expression through the application of different promoters and inducers, ranging from weakly expressed *clsA* in uninduced RJ118b to a situation where the gene was very strongly expressed by the addition of thiostrepton to RJ110, had a dramatic effect on both substrate hyphae and aerial hyphae. Increasing the strength of the promoter from which *clsA* was transcribed increased hyphal width and the frequency with which branching occurred. Surprisingly, increasing the expression of *clsA* also caused changes in direction of the hyphal tip; in conditions where *clsA* was depleted (uninduced RJ118b), extending hyphal tips changed direction less frequently and at a less acute angle than the wild-type strain. Under conditions when *clsA* was overexpressed (induced RJ110), extending hyphal tips changed direction more frequently and at a more acute angle than the wild-type strain. This suggests that, perhaps due to the conical structure of CL and its capacity to associate into clusters (Huang *et al.*, 2006), CL may play a role in the introduction of bends in an extending hypha. It may be that CL is responsible for the direct introduction of hyphal bends or perhaps this effect is mediated by a cytoskeletal protein such

as MreB (Mazza *et al.*, 2006) or FilP (Bagchi *et al.*, 2008). Time-lapse microscopy was used to demonstrate the weakened nature of the hyphal tips when *clsA* was overexpressed and this was shown by their capacity to lyse at the hyphal tip and undergo a splitting of the tip rather than branching that generally takes place some distance from the hyphal tip (Jyothikumar *et al.*, 2008). Although it was not possible to observe the effects of depleting *clsA* on sporulation due to the dependence of erection of aerial hyphae on expression of this gene, overexpression led to aberrant aerial hyphae showing regions of PL enrichment that often coincided with regions of peptidoglycan incorporation. Liquid-grown cultures of *S. coelicolor* show colocalization of FM4–64 and vancomycin-FL staining (Manteca *et al.*, 2008) and suggests that there may be an association of clusters enriched in certain PLs and peptidoglycan incorporation in this organism. Under conditions of *clsA* overexpression, many aerial hyphae did not mature to generate spores; however, when they did so, most of the spores were anucleate. As staining of substrate hyphae with NAO and Syto42 showed that the location of CL and nucleoids were mutually exclusive it is perhaps unsurprising that increasing the levels of CL in aerial hyphae should reduce the proportion of prespores occupied by nucleoids. Nevertheless, the reciprocal relationship of nucleoid staining with CL staining suggests that nucleoid position is somehow either linked to regions of CL enrichment through the nucleoids themselves or perhaps mediated through nucleoid-associated proteins (Jakimowicz *et al.*, 2005; Ruban-Osmialowska *et al.*, 2006; Zakrzewska-Czerwinska *et al.*, 2007; Wolanski *et al.*, 2011).

Protein association with CL-enriched clusters at the poles of unicellular bacteria (Mileykovskaya and Dowhan, 2009) suggests that such regions may recruit tip-associated proteins in *Streptomyces* and so might explain the increase in branching frequency in response to changes in *clsA* expression. For example, *S. coelicolor*, DivIVA is localized at hyphal tips and is recruited to future branch points before branch emergence from the primary hypha (Flardh, 2003a,b, Hempel *et al.*, 2008), while CslA, which interacts with DivIVA (Xu *et al.*, 2008), and TraB (Reuther *et al.*, 2006) are also located at the hyphal tip. It is not known what directs these proteins to tips and future branch sites (Flardh and Buttner, 2009), although the localization of CL to the tip means that the anionic properties of CL might provide a means to recruit these proteins to specific membrane regions or these proteins might target the intrinsic negative curvature of the hyphal tip itself (Lenarcic *et al.*, 2009).

Although we were unable to observe ClsA-EGFP localization to discrete hyphal regions, with the possible exception of the base of aerial hyphae, CL associated to form enriched clusters when *S. coelicolor* was stained with NAO. Areas of staining corresponded to tips and branch points. Taken together this suggests that ClsA is not restricted to specific hyphal locations, and as such, CL synthesis is similarly ubiquitously located in substrate hyphae. CL, on the other hand is concentrated in specific regions that correspond to membrane regions such as hyphal tips and branch points. This observation is consistent with mathematically derived predictions that it is energetically favourable for CL to associate in curved membrane regions (Huang *et al.*, 2006; Renner and Weibel, 2011). The corollary of this is that CL association to form regions of enrichment may be an emergent property of filamentous bacteria that allows branching. Changing the level of expression of *clsA* results in changes in branching frequency and hyphal bending and, while it is not possible to be certain of cause and effect, this finding suggests that CL may play a role in controlling mycelial architecture through the recruitment of cytokinetic proteins to sites of hyphal extension and branching.

In summary, we have described the contribution of the phospholipid CL to morphogenesis in *S. coelicolor* and demonstrated that although ClsA is not localized to specific hyphal regions, CL forms sites of enrichment at hyphal tips and branch points. By regulating

expression of *clsA* we were able to influence the mycelial architecture of this organism. It will be intriguing to determine whether this effect is mediated either directly or indirectly through interaction with protein partners.

Experimental procedures

Bacterial strains and media

Escherichia coli strains were cultivated in Luria–Bertani solid and liquid medium (250 r.p.m.) at 37°C, while *S. coelicolor* strains were grown on MS agar for propagation or minimal agar containing 5% (w/v) mannitol (3MA) for microscopy or PL extraction (Kieser *et al.*, 2000). *S. coelicolor* liquid cultures were grown in YEME in baffled flasks at 275 r.p.m. (Kieser *et al.*, 2000). Where appropriate, medium was supplemented with 100 μg ml^{-1} apramycin (am), 25 μg ml^{-1} kanamycin (km), 20 μg ml^{-1} nalidixic acid (nal), 50 μg ml^{-1} hygromycin (hyg), 50 μg ml^{-1} ampicillin (ap), 12.5 μg ml^{-1} tetracycline (tet), 25 μg ml^{-1} chloramphenicol (cm), 25 μg ml^{-1} thiostrepton (tsr) or 1.5 μg ml^{-1} anhydrotetracycline (atc). Plasmids and mutated cosmids were introduced into *S. coelicolor* by intergeneric conjugation from *E. coli* ET12567(pUZ8002) and transconjugants identified using appropriate antibiotics (Kieser *et al.*, 2000). All plasmids and bacterial strains are described in Table 1. *Streptomyces* genomic DNA was used to confirm strains by Southern analysis using appropriate digoxigenin-labelled probes (Kieser *et al.*, 2000).

Generation of *clsA* mutant strains of *S. coelicolor*

Cloning procedures and strain verification by Southern blotting were performed using standard procedures (Sambrook and Russel, 1989; Kieser *et al.*, 2000). PCR conditions were performed under standard conditions using Pfu DNA polymerase (Stratagene) and primers are listed in Table S3. To facilitate complementation, *clsA* was cloned from SC1A8A.2.EO5 on a 4136 bp EcoRI fragment into pALTER1 generating pCLS102. *clsA* was then cloned from this plasmid into pMS82 (Gregory *et al.*, 2003) as a 1593 bp HindIII fragment. The resulting plasmid, pCLS105, allowed *clsA* to be delivered to $attB_{\Phi BT1}$ for complementation of *clsA* null mutants. In order to disrupt *clsA*, we introduced the transposed cosmid SC1A8A.2.B10, a cosmid from the transposon mutant ordered cosmid library of *S. coelicolor* (Bishop *et al.*, 2004; Herron *et al.*, 2004; Fernandez-Martinez *et al.*, 2011) carrying *clsA* disrupted with the minitransposon Tn*5062*, into *S. coelicolor* M145 by conjugation from *E. coli* ET12567(pUZ8002). The PCR-targeting procedure of Gust *et al.* (2003) was used to replace *clsA* in cosmid SC1A8A (Redenbach *et al.*, 1996) with the apramycin resistance gene, *aac(3)IV* (*am*^{r}), amplified with primers CL104 and CL105 designed so that the 5′-ends were homologous to sequences flanking *clsA*. The resulting PCR product was used to replace *clsA* with *am*^{r} creating SC1A8AΔ*clsA*. A transconjugant that carried SC1A8AΔ*clsA* integrated in the M145 chromosome via a single recombination event was termed RJ111 and, following the conjugation of this strain with *E. coli* ET12567(pUZ8002) carrying pCLS105, we obtained RJ114 (hyg^r am^r km^s) that had undergone a deletion of the parental copy of *clsA* and carried a second copy of *clsA* (from pCLS105) integrated at $attP_{\Phi BT1}$ (Fig. 1).

A plasmid that would allow the depletion of *clsA* was constructed using pAV11B (Khaleel *et al.*, 2011). pAV11B contains the *tcp830* promoter and *tetris* cassette (Rodriguez-Garcia *et al.*, 2005) in pMS82 (Gregory *et al.*, 2003). Consequently genes placed downstream of the *tcp830* promoter are subject to repression by TetRis and can be de-repressed by addition of tetracycline inducers such as atc. This plasmid integrates at $attP_{\Phi BT1}$ (Gregory *et al.*, 2003). *clsA* was amplified from plasmid pCLS105 using primers CL102 and CL103, digested with XbaI and EcoRV; the resulting 673 bp *clsA*-containing band was gel purified and end-filled with Klenow enzyme generating a blunt ended fragment which was cloned into the EcoRV

site of pAVIIB generating pCLS117B1. A strain that had undergone an allelic replacement via a double recombination event, RJ118b (hyg^r am^r km^s), was obtained when pAV117B1 was transferred via conjugation from *E. coli* ET12567(pUZ8002) to RJ111 when the agar was supplemented with atc.

A translational fusion of ClsA to EGFP was created by amplifying *clsA* from pCLS105 using the primers CL100 and CL101. The PCR product was digested with BamHI and XbaI and cloned into BamHI- and NheI-digested pEGFP-N1 generating pCLS107. This plasmid was digested with VspI and PvuII allowing *clsA-egfp* to be cloned into VspI- and EcoRV-digested pMS82 creating pCLS108B.

pCLS113A, a plasmid allowing the overexpression of *clsA*, was constructed by fusing it to the thiostrepton-inducible promoter (*ptipA*). *clsA* was first amplified from pCLS105 using primers CL102 and CL103, digested with NdeI and XbaI and cloned into the NdeI and XbaI sites of pIJ8600 (Sun *et al.*, 1999) generating pCLS113A, with *clsA* placed downstream of *ptipA*.

Semi-quantitative RT-PCR

Streptomyces coelicolor mycelium grown on cellophane discs was harvested from 2-day-old 3MA plates with a sterile razor blade and immediately added to two volumes of RNA protect Bacteria Reagent (Qiagen), vortexed for 5 s and incubated for 5 min at room temperature. After centrifugation at 13000 r.p.m. for 10 min, the supernatant fraction was incubated with 200 μl of lysozyme (3 mg ml^{-1}) in TE buffer for 30 min. After addition of 700 μl of RLT buffer (Qiagen) and centrifugation for 5 min, the supernatant fraction was mixed with 1 volume of phenol/chloroform, inverted five times and centrifuged for 5 min at 13000 r.p.m. After a second phenol extraction of the upper aqueous phase, the latter was further purified using a Qiagen RNeasy kit according to the manufacturer's instructions. RNA was analysed with a Nanodrop ND-1000 (Thermo Fischer Scientific) for quantity and quality and stored at −80°C in aliquots. RNase free DNase I (Qiagen) was used to remove contaminating DNA (37°C, 30 min) followed by DNase I inactivation (75°C, 10 min). RT-PCR was carried out with 100 ng of RNA using the Qiagen One-Step RT-PCR kit according to the manufacturer's instructions in a Biorad PTC-100 DNA Engine. After reverse transcription (50°C, 30 min) and subsequent inactivation of reverse transcriptase (95°C, 15 min) the PCR was carried according to the following conditions: denaturation, 94°C, 30 s; annealing 60°C, 30 s; extension, 72°C, 1 min for 30 cycles followed by a final extension at 72°C for 10 min. Primers *SCO1389*_F and *SCO1389*_R were used to amplify *clsA* while *hrdB*_F and *hrdB*_R were used to amplify the internal control, *hrdB* (Table S3). Samples were analysed by agarose gel electrophoresis and bands quantified by densitometry using the Genetools software package (Syngene).

Extraction and development of PLs and analysis of PLs using electrospray mass spectrometry

Streptomyces coelicolor mycelium grown on cellophane discs was harvested from 2-day-old 3MA plates with a sterile razor blade or from liquid cultures by centrifugation (13000 r.p.m., 5 min) of 1.5 ml of culture broth. In either case, PLs were extracted from mycelial pellets (100 mg, wet weight; equivalent to 27 mg dry weight of mycelium) by resuspension in 100 μl of chloroform, 200 μl of methanol and 80 μl of water before vortexing for 10 min. Another 100 μl of chloroform was added and the sample vortexed for a further minute. One hundred microlitres of water was then added to the sample and vortexed for 1 min. Centrifugation at 13000 r.p.m. for 1 min. caused the phases to separate, with the mycelial fragments forming a disc which divided the upper (aqueous) and lower (organic) phases. The lower phase was carefully removed and evaporated to dryness in a vacuum centrifuge

(Bligh and Dyer, 1959). Residues were stored at −80°C until analysed by TLC or electrospray mass spectrometry.

For TLC analysis, each residue was resuspended in 3 μl of chloroform just prior to applying to a 250 μm thickness 200 mm × 200 mm K6 60A porosity silica gel TLC plate (Fisher). PL standards (Sigma) dissolved in ethanol (5 μg each) were also applied to TLC plates to aid identification of unknown spots: α-phosphatidyl-$_{DL}$-glycerol, sodium salt from egg yolk lecithin (PG) (primarily C34); 3-snphosphatidylethanolamine (PE) from bovine brain (primarily C38:5) and CL solution from bovine heart (CL) (primarily C72:8). TLC plates were developed in chloroform/methanol/acetic acid/water (80:12:15:4) and PLs visualized by spraying with molybdenum blue spray reagent (Sigma).

Aliquots of total lipid extracts were analysed with a Micromass Quattro Ultima triple quadrupole mass spectrometer equipped with a nanoelectrospray source. Samples were loaded into thin-wall nanoflow capillary tips (Waters) and analysed by ES-MS in both positive and negative ion modes using a capillary voltage of 0.9 kV and cone voltages of 50 V. MS/MS daughter ion scanning was performed using argon as the collision gas (~ 3.0 mTorr) with collision energies between 35 and 70 V CL species were detected by precursor scanning for m/z 153 in negative ion mode between 600 and 100 m/z and 1000 and 2000 m/z with a collision energy ~ 70 V. CL species were assigned according to their daughter ion fragments: $[PA\text{-}H]^-$, $[lysoPA\text{-}H]^-$ or $[lysoPA\text{-}H_2O\text{-}H]^-$ and fatty acids based on their $[M\text{-}H]^-$ values. Each spectrum encompasses at least 50 repetitive scans. The identity of phospholipid peaks was verified using the Lipid Molecular Structure Database (http://www.lmsd.tcd.ie/) (Sud *et al.*, 2007).

Fluorescence microscopy

Imaging chambers were prepared as previously described (Jyothikumar *et al.*, 2008). Briefly, cellophane squares were placed on sterile coverslips and inserted into 3MA at an acute angle before inoculation with around 1×10^7 *S. coelicolor* spores (Schwedock *et al.*, 1997). After 36 h, the cellophane was peeled away from the coverslip and transferred to imaging chambers. (IBIDI GmbH). Where appropriate, FM4-64 (5 ng μl^{-1}), Syto42 (1 μM) and Vancomycin-FL (1 ng μl^{-1}) were added to 3MA plugs cut with a number 4 cork borer. Figures in parentheses represent the final concentration of the dyes in the plug. After equilibration for 30 min in the dark, the plug was placed on top of the cellophane and allowed to equilibrate for a further 15 min to allow diffusion of the dyes through the cellophane to stain the hyphae. For time-lapse microscopy of growth of substrate hyphae, spores were germinated on 0.5 cm^2 sterile cellophane squares, placed on 3MA and incubated at 30°C. Cellophane was removed after an appropriate time intervals and transferred to imaging chambers and heated to 30°C for 60 min before imaging commenced (Jyothikumar *et al.*, 2008). For visualization of CL enriched membrane domains and nucleoids, NAO (100 ng μl^{-1}) and Syto42 (1 μM) were added to 40% (w/v) glycerol in PBS and 8 μl added directly to coverslip-grown hyphae before sealing and imaging within 30 min to ensure hyphal viability. Staining of nucleoids with Propidium iodide and FITC-WGA (newly synthesized peptidoglycan) was carries out according to Schwedock *et al.* (1997). All stains were purchased from Invitrogen.

Samples were viewed with a Nikon TE2000S inverted microscope and observed with a CFI Plan Fluor DLL-100× oil N.A. 1.3 objective lens and captured using a Hamamatsu Orca-285 Firewire Digital CCD Camera. Captured images were processed using IPlabs 3.7 image processing software (BD Biosciences Bioimaging, Rockville, Maryland, USA). ClsA-EGFP in *S. coelicolor* RJ113 and Vancomycin-FL were visualized with a FITC filter (Ex 492/18; Em 520/20), Syto42 with a DAPI filter set (Ex 403/12; Em 455/10) and FM4-64 with a TRITC filter set (Ex 572/23; Em 600/20). NAO staining of anionic PLs in general was

visualized with a FITC filter set and staining of CL visualized with a TRITC filter set (Mileykovskaya and Dowhan, 2000).

Measurements of morphological parameters were made using IPlabs 3.7 image processing software and analysed statistically using Microsoft Excel 2003; equality of variance between data sets was first determined using *F*-tests and then subjected to the appropriate Student's *t*-test depending on the outcome of the *F*-test. Multiple data sets were analysed by analysis of variance (ANOVA). Where appropriate, means are supplemented by standard deviations.

Supplementary Material

Refer to Web version on PubMed Central for supplementary material.

Acknowledgments

We are grateful to Dr Anpu Varghese and Professor Maggie Smith (University of Aberdeen) for the provision of pAV11B. V.J. and J.T. were supported by Faculty of Science Scholarships from the University of Strathclyde and K.K. by a Scholarship from the Royal Thai Government. We would like to thank Dr Corinne Spickett (University of Aston) for critical reading of this manuscript. The Strathclyde group were supported by a BBSRC grant awarded to PRH (BB/D521657/1). TKS was supported by a Wellcome Trust Senior Research Fellowship (067441) and Wellcome Trust project grants (086658 and 093228).

References

Ali N, Herron PR, Evans MC, Dyson PJ. Osmotic regulation of the *Streptomyces lividans* thiostrepton-inducible promoter, ptipA. Microbiology. 2002; 148:381–390. [PubMed: 11832502]

Bagchi S, Tomenius H, Belova LM, Ausmees N. Intermediate filament-like proteins in bacteria and a cytoskeletal function in *Streptomyces*. Mol Microbiol. 2008; 70:1037–1050. [PubMed: 18976278]

Barak I, Muchova K, Wilkinson AJ, O'Toole PJ, Pavlendova N. Lipid spirals in *Bacillus subtilis* and their role in cell division. Mol Microbiol. 2008; 68:1315–1327. [PubMed: 18430139]

Bishop A, Fielding S, Dyson P, Herron P. Systematic insertional mutagenesis of a streptomycete genome: a link between osmoadaptation and antibiotic production. Genome Res. 2004; 14:893–900. [PubMed: 15078860]

Bligh EG, Dyer WJ. A rapid method of total lipid extraction and purification. Can J Biochem Physiol. 1959; 37:911–917. [PubMed: 13671378]

Borodina I, Krabben P, Nielsen J. Genomescale analysis of *Streptomyces coelicolor* A3(2) metabolism. Genome Res. 2005; 15:820–829. [PubMed: 15930493]

Daniel RA, Errington J. Control of cell morphogenesis in bacteria: two distinct ways to make a rod-shaped cell. Cell. 2003; 113:767–776. [PubMed: 12809607]

Fernandez-Martinez LT, Del Sol R, Evans MC, Fielding S, Herron PR, Chandra G, Dyson PJ. A transposon insertion single-gene knockout library and new ordered cosmid library for the model organism *Streptomyces coelicolor* A3(2). Antonie Van Leeuwenhoek. 2011; 99:515–522. [PubMed: 20945092]

Flardh K. Essential role of DivIVA in polar growth and morphogenesis in *Streptomyces coelicolor* A3(2). Mol Microbiol. 2003a; 49:1523–1536. [PubMed: 12950918]

Flardh K. Growth polarity and cell division in *Streptomyces*. Curr Opin Microbiol. 2003b; 6:564–571. [PubMed: 14662351]

Flardh K, Buttner MJ. *Streptomyces* morphogenetics: dissecting differentiation in a filamentous bacterium. Nat Rev Microbiol. 2009; 7:36–49. [PubMed: 19079351]

Gregory MA, Till R, Smith MCM. Integration site for *Streptomyces* phage phiBT1 and development of site-specific integrating vectors. J Bacteriol. 2003; 185:5320–5323. [PubMed: 12923110]

Gust B, Challis GL, Fowler K, Kieser T, Chater KF. PCR-targeted *Streptomyces* gene replacement identifies a protein domain needed for biosynthesis of the sesquiterpene soil odor geosmin. Proc Natl Acad Sci USA. 2003; 100:1541–1546. [PubMed: 12563033]

Europe PMC Funders Author Manuscripts

Hempel AM, Wang SB, Letek M, Gil JA, Flardh K. Assemblies of DivIVA mark sites for hyphal branching and can establish new zones of cell wall growth in *Streptomyces coelicolor*. J Bacteriol. 2008; 190:7579–7583. [PubMed: 18805980]

Herron PR, Hughes G, Chandra G, Fielding S, Dyson PJ. Transposon Express, a software application to report the identity of insertions obtained by comprehensive transposon mutagenesis of sequenced genomes: analysis of the preference for *in vitro* Tn5 transposition into GC-rich DNA. Nucleic Acids Res. 2004; 32:e113. [PubMed: 15308758]

Hoischen C, Gura K, Luge C, Gumpert J. Lipid and fatty acid composition of cytoplasmic membranes from *Streptomyces hygroscopicus* and its stable protoplast-type L form. J Bacteriol. 1997; 179:3430–3436. [PubMed: 9171384]

Huang KC, Mukhopadhyay R, Wingreen NS. A curvature-mediated mechanism for localization of lipids to bacterial poles. PLoS Comput Biol. 2006; 2:1357–1364.

Jackson M, Crick DC, Brennan PJ. Phosphatidylinositol is an essential phospholipid of mycobacteria. J Biol Chem. 2000; 275:30092–30099. [PubMed: 10889206]

Jakimowicz D, Gust B, Zakrzewska-Czerwinska J, Chater KF. Developmental-stage-specific assembly of ParB complexes in *Streptomyces coelicolor* hyphae. J Bacteriol. 2005; 187:3572–3580. [PubMed: 15866947]

Jyothikumar V, Tilley EJ, Wali R, Herron PR. Time-lapse microscopy of *Streptomyces coelicolor* growth and sporulation. Appl Environ Microbiol. 2008; 74:6774–6781. [PubMed: 18791015]

Kawai F, Shoda M, Harashima R, Sadaie Y, Hara H, Matsumoto K. Cardiolipin domains in *Bacillus subtilis* Marburg membranes. J Bacteriol. 2004; 186:1475–1483. [PubMed: 14973018]

Khaleel T, Younger E, McEwan AR, Varghese AS, Smith MCM. A phage protein that binds phi C31 integrase to switch its directionality. Mol Microbiol. 2011; 80:1450–1463. [PubMed: 21564337]

Kieser, T.; Bibb, MJ.; Buttner, MJ.; Chater, KF.; Hopwood, DA. Practical Streptomyces Genetics. John Innes Foundation; Norwich: 2000.

Lenarcic R, Halbedel S, Visser L, Shaw M, Wu LJ, Errington J, et al. Localisation of DivIVA by targeting to negatively curved membranes. EMBO J. 2009; 28:2272–2282. [PubMed: 19478798]

Limonet M, Saffroy S, Maujean F, Linder M, Delaunay S. A comparison of disruption procedures for the analysis of phospholipids from *Streptomyces pristinaespiralis*. Process Biochem. 2007; 42:700–703.

Manteca A, Alvarez R, Salazar N, Yague P, Sanchez J. Mycelium differentiation and antibiotic production in submerged cultures of *Streptomyces coelicolor*. Appl Environ Microbiol. 2008; 74:3877–3886. [PubMed: 18441105]

Matsumoto K, Kusaka J, Nishibori A, Hara H. Lipid domains in bacterial membranes. Mol Microbiol. 2006; 61:1110–1117. [PubMed: 16925550]

Mazza P, Noens EE, Schirner K, Grantcharova N, Mommaas AM, Koerten HK, et al. MreB of *Streptomyces coelicolor* is not essential for vegetative growth but is required for the integrity of aerial hyphae and spores. Mol Microbiol. 2006; 60:838–852. [PubMed: 16677297]

Mileykovskaya E, Dowhan W. Visualization of phospholipid domains in *Escherichia coli* by using the cardiolipin-specific fluorescent dye 10-N-nonyl acridine orange. J Bacteriol. 2000; 182:1172–1175. [PubMed: 10648548]

Mileykovskaya E, Dowhan W. Role of membrane lipids in bacterial division-site selection. Curr Opin Microbiol. 2005; 8:135–142. [PubMed: 15802243]

Mileykovskaya E, Dowhan W. Cardiolipin membrane domains in prokaryotes and eukaryotes. Biochim Biophys Acta. 2009; 1788:2084–2091. [PubMed: 19371718]

Morita YS, Englund PT. Fatty acid remodeling of glycosyl phosphatidylinositol anchors in *Trypanosoma brucei*: incorporation of fatty acids other than myristate. Mol Biochem Parasitol. 2001; 115:157–164. [PubMed: 11420102]

Nodwell JR, McGovern K, Losick R. An oligopeptide permease responsible for the import of an extracellular signal governing aerial mycelium formation in *Streptomyces coelicolor*. Mol Microbiol. 1996; 22:881–893. [PubMed: 8971710]

Redenbach M, Kieser HM, Denapaite D, Eichner A, Cullum J, Kinashi H, Hopwood DA. A set of ordered cosmids and a detailed genetic and physical map for the 8 Mb *Streptomyces coelicolor* A3(2) chromosome. Mol Microbiol. 1996; 21:77–96. [PubMed: 8843436]

Renner LD, Weibel DB. Cardiolipin microdomains localize to negatively curved regions of *Escherichia coli* membranes. Proc Natl Acad Sci USA. 2011; 108:6264–6269. [PubMed: 21444798]

Reuther J, Gekeler C, Tiffert Y, Wohlleben W, Muth G. Unique conjugation mechanism in mycelial streptomycetes: a DNA-binding ATPase translocates unprocessed plasmid DNA at the hyphal tip. Mol Microbiol. 2006; 61:436–446. [PubMed: 16776656]

Rodriguez-Garcia A, Combes P, Perez-Redondo R, Smith MCA, Smith MCM. Natural and synthetic tetracycline-inducible promoters for use in the antibiotic-producing bacteria *Streptomyces*. Nucleic Acids Res. 2005; 33:e87. [PubMed: 15917435]

Romantsov T, Helbig S, Culham DE, Gill C, Stalker L, Wood JM. Cardiolipin promotes polar localization of osmosensory transporter ProP in *Escherichia coli*. Mol Microbiol. 2007; 64:1455–1465. [PubMed: 17504273]

Romantsov T, Stalker L, Culham DE, Wood JM. Cardiolipin controls the osmotic stress response and the subcellular location of transporter ProP in *Escherichia coli*. J Biol Chem. 2008; 283:12314–12323. [PubMed: 18326496]

Ruban-Osmialowska B, Jakimowicz D, Smulczyk-Krawczyszyn A, Chater KF, Zakrzewska-Czerwinska J. Replisome localization in vegetative and aerial hyphae of *Streptomyces coelicolor*. J Bacteriol. 2006; 188:7311–7316. [PubMed: 17015671]

Sambrook, J.; Russel, DW. Molecular Cloning: A Laboratory Manual. Cold Spring Harbor Laboratory Press; Cold Spring Harbor, NY: 1989.

Sandoval-Calderon M, Geiger O, Guan ZQ, Barona-Gomez F, Sohlenkamp C. A eukaryote-like cardiolipin synthase is present in *Streptomyces coelicolor* and in most actinobacteria. J Biol Chem. 2009; 284:17383–17390. [PubMed: 19439403]

Schlame M, Rua D, Greenberg ML. The biosynthesis and functional role of cardiolipin. Prog Lipid Res. 2000; 39:257–288. [PubMed: 10799718]

Schwedock J, McCormick JR, Angert ER, Nodwell JR, Losick R. Assembly of the cell division protein FtsZ into ladder-like structures in the aerial hyphae of *Streptomyces coelicolor*. Mol Microbiol. 1997; 25:847–858. [PubMed: 9364911]

Singer SJ, Nicolson GL. The fluid mosaic model of the structure of cell membranes. Science. 1972; 175:720–731. [PubMed: 4333397]

Sud M, Fahy E, Cotter D, Brown A, Dennis EA, Glass CK, et al. LMSD: LIPID MAPS structure database. Nucleic Acids Res. 2007; 35:D527–D532. [PubMed: 17098933]

Sun JH, Kelemen GH, Fernandez-Abalos JM, Bibb MJ. Green fluorescent protein as a reporter for spatial and temporal gene expression in *Streptomyces coelicolor* A3(2). Microbiology. 1999; 145:2221–2227. [PubMed: 10517575]

Willey JM, Willems A, Kodani S, Nodwell JR. Morphogenetic surfactants and their role in the formation of aerial hyphae in *Streptomyces coelicolor*. Mol Microbiol. 2006; 59:731–742. [PubMed: 16420347]

Wolanski M, Wali R, Tilley E, Jakimowicz D, Zakrzewska-Czerwinska J, Herron P. Replisome trafficking in growing vegetative hyphae of *Streptomyces coelicolor* A3(2). J Bacteriol. 2011; 193:1273–1275. [PubMed: 21193604]

Xu HB, Chater KF, Deng ZX, Tao MF. A cellulose synthase-like protein involved in hyphal tip growth and morphological differentiation in *Streptomyces*. J Bacteriol. 2008; 190:4971–4978. [PubMed: 18487344]

Zakrzewska-Czerwinska J, Jakimowicz D, Zawilak-Pawlik A, Messer W. Regulation of the initiation of chromosomal replication in bacteria. FEMS Microbiol Rev. 2007; 31:378–387. [PubMed: 17459114]

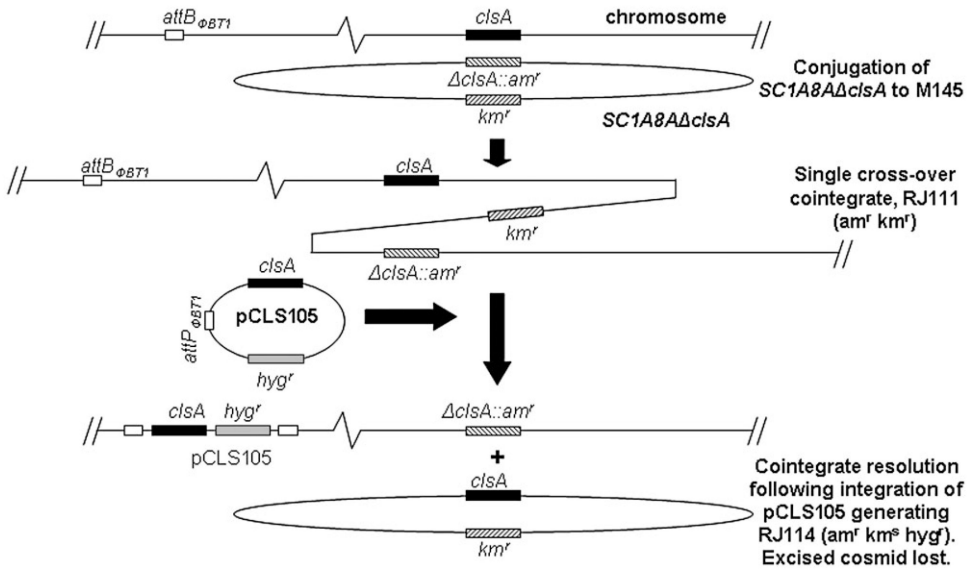

Fig. 1.

Integration and excision of SC1A8AΔ*clsA* following complementation with pCLS105. Isolation of am^r, km^r transconjugants (where the entire deletion vector (SC1A8AΔ*clsA*) had integrated into the chromosome via a single recombination event) was carried out according to (Gust *et al.*, 2003) resulting in RJ111. Following complementation of this strain with a second copy of *clsA* carried on pCLS105, transconjugant colonies that had undergone replacement of parental *clsA* with Δ*clsA::am*^{r} were then isolated (RJ114, am^r, km^s, hyg^r). RJ118b (am^r, km^s, hyg^r) was generated in the same way as RJ114 after introduction of pAV117B1 except that atc was also incorporated into the agar.

Europe PMC Funders Author Manuscripts

Europe PMC Funders Author Manuscripts

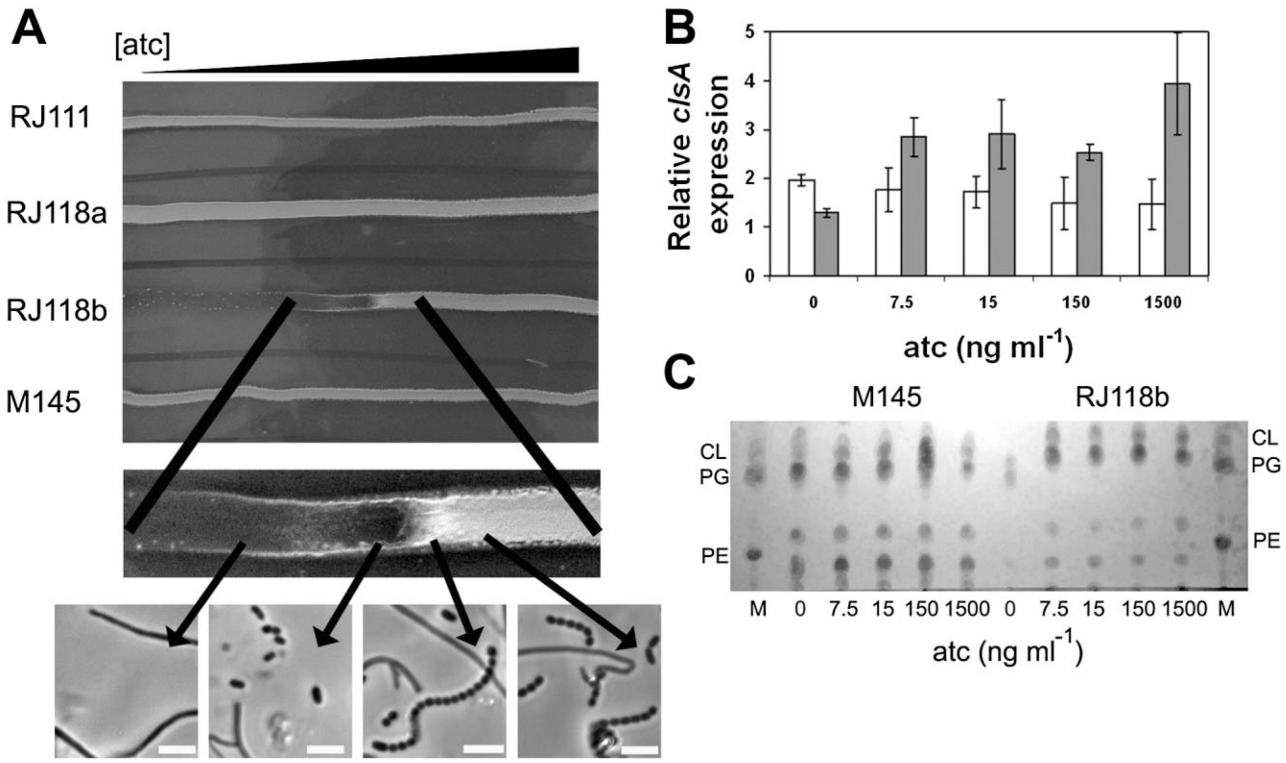

Fig. 2.

Effect of reduction of *clsA* expression on *S. coelicolor* morphogenesis.

A. Spores of RJ111, RJ118a, RJ118b and M145 were plated on 3MA along a gradient of atc (0–1.5 μg ml^{-1}). An impression of growth at the boundary between substrate and aerial growth was made by placing a coverslip across the boundary that was subsequently examined by phase-contrast microscopy. Horizontal white bars represent 5 μm.

B. Cultures of M145 (open bars) and RJ118b (hatched bars) were grown on cellophane discs on 3MA in the presence of 0, 7.5, 15, 150 and 1500 ng ml^{-1} atc for 48 h before extraction of RNA and analysis of *clsA* expression by semi quantitative RT-PCR. After RNA isolation and cDNA synthesis, transcript levels were compared by RT-PCR with that of the internal control (*hrdB*). Three biological replicates of the RT-PCR were carried out; all showed similar patterns of *clsA* expression from M145 and atc-dependent *clsA* expression from RJ118b. Bands were quantified by densitometry and related to the *hrdB* internal standard (see *Experimental procedures*). These data are displayed as a histogram. Error bars represent standard deviation.

C. Phospholipids were extracted from 100 mg of M145 and RJ118b mycelia grown in the presence of 0, 7.5, 15, 150 and 1500 ng ml^{-1} atc for 48 h and scraped from 3MA plates and developed by TLC (see *Experimental procedures*). M, marker of PL standards: cardiolipin, CL; phosphatidylglycerol, PG; and phosphatidylethanolamine, PE (each 5 μg).

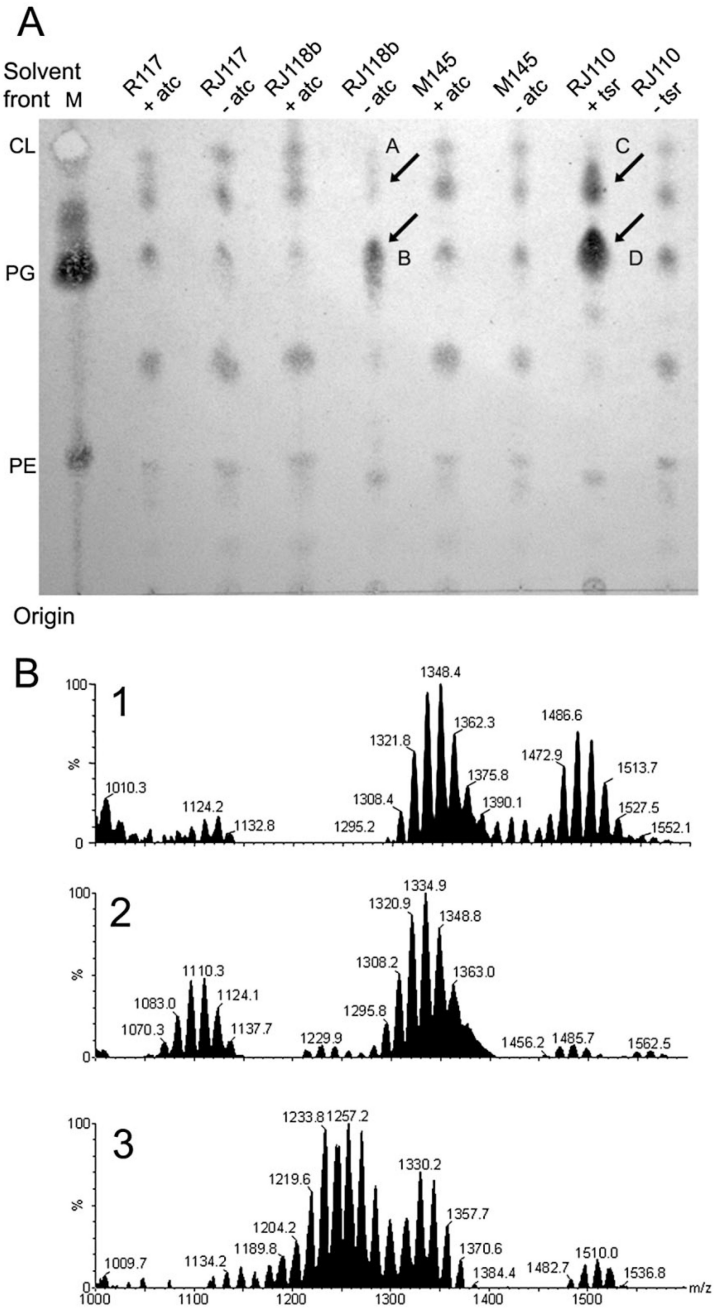

Fig. 3.

Depletion of *clsA* causes an altered PL profile.

A. TLC of PLs from liquid-grown mid-log phase *S. coelicolor* RJ117 (lanes 1 and 2), RJ118b (lanes 3 and 4), M145 (lanes 5 and 6) and RJ110 (lanes 7 and 8) grown in YEME in the presence of 1.5 μg ml^{-1} atc (lanes 1, 3 and 5) or 100 μM thiostrepton (lane 7) after PL and TLC (see *Experimental procedures*). PLs that differed between the strains are labelled (A–D). M, marker of PL standards: cardiolipin, CL; phosphatidylglycerol, PG; and phosphatidylethanolamine, PE (each 5 μg).

B. Negative ion ES-MS survey scans (1000–1600 m/z) of total lipid extracts from M145 (1) and RJ118b in the absence (2) or presence (3) of 1.5 μg ml^{-1} atc.

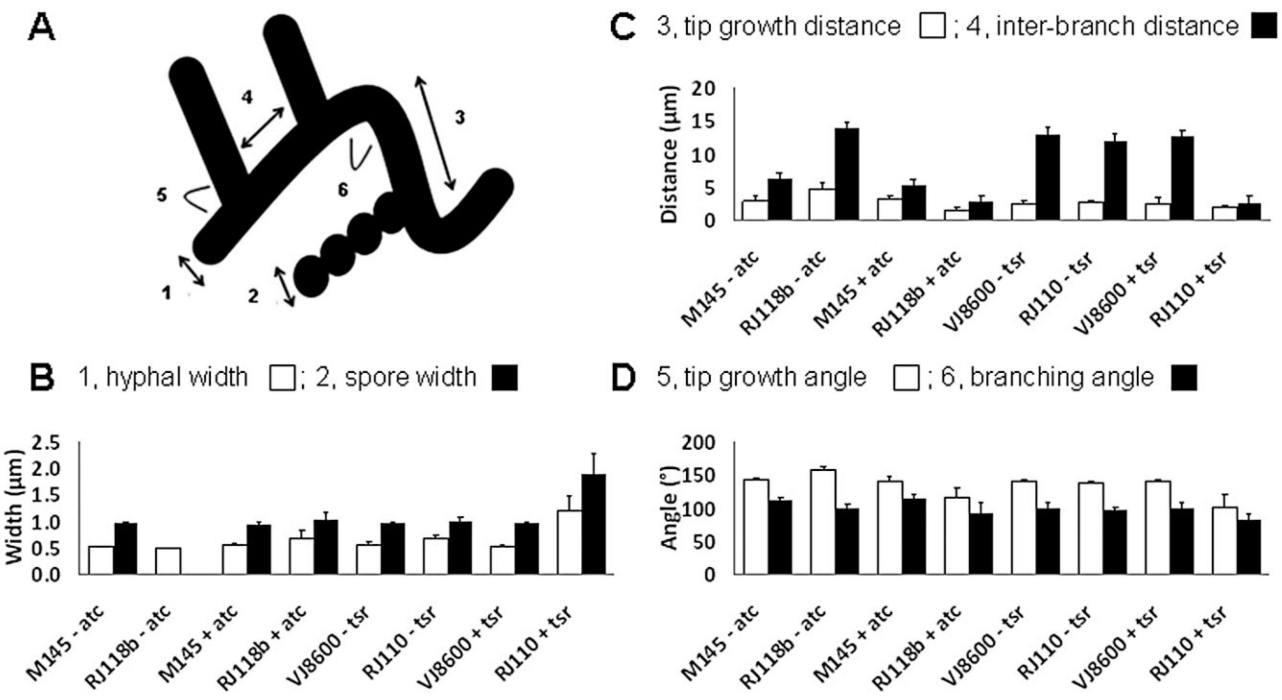

Fig. 4.

Alteration of *clsA* expression affects hyphal growth and branching. Hyphae of M145 (− atc, $n = 83$; + atc, $n = 75$), RJ118b (− atc, $n = 60$; + atc, $n = 88$), VJ8600 (− tsr $n = 69$; + tsr, $n = 74$) and RJ110 (− tsr, $n = 74$; + tsr, $n = 108$) were grown in the absence and presence of 1.5 µg ml^{-1} atc or 100 µM thiostrepton (tsr) and a number of parameters that quantitatively describe mycelial architecture (A) were measured and their means are presented as histograms.

A. The cartoon shows graphically how these parameters relate to a streptomycete mycelium. B–D. (B) 1, hyphal width (µm, open bars); 2, spore width (µm, closed bars). (C) 3, tip growth distance (the distance between changes in tip direction) (µm, open bars); 4, inter-branch distance (µm, closed bars). (D) 5 tip growth angle (the angle which a hypha was bent following a change in tip growth direction) (°, open bars); 6, branching angle (°, closed bars). Error bars represent standard deviation of the mean. Actual figures are given in supplementary Table S1 and the results of tests of significance given in Table S2.

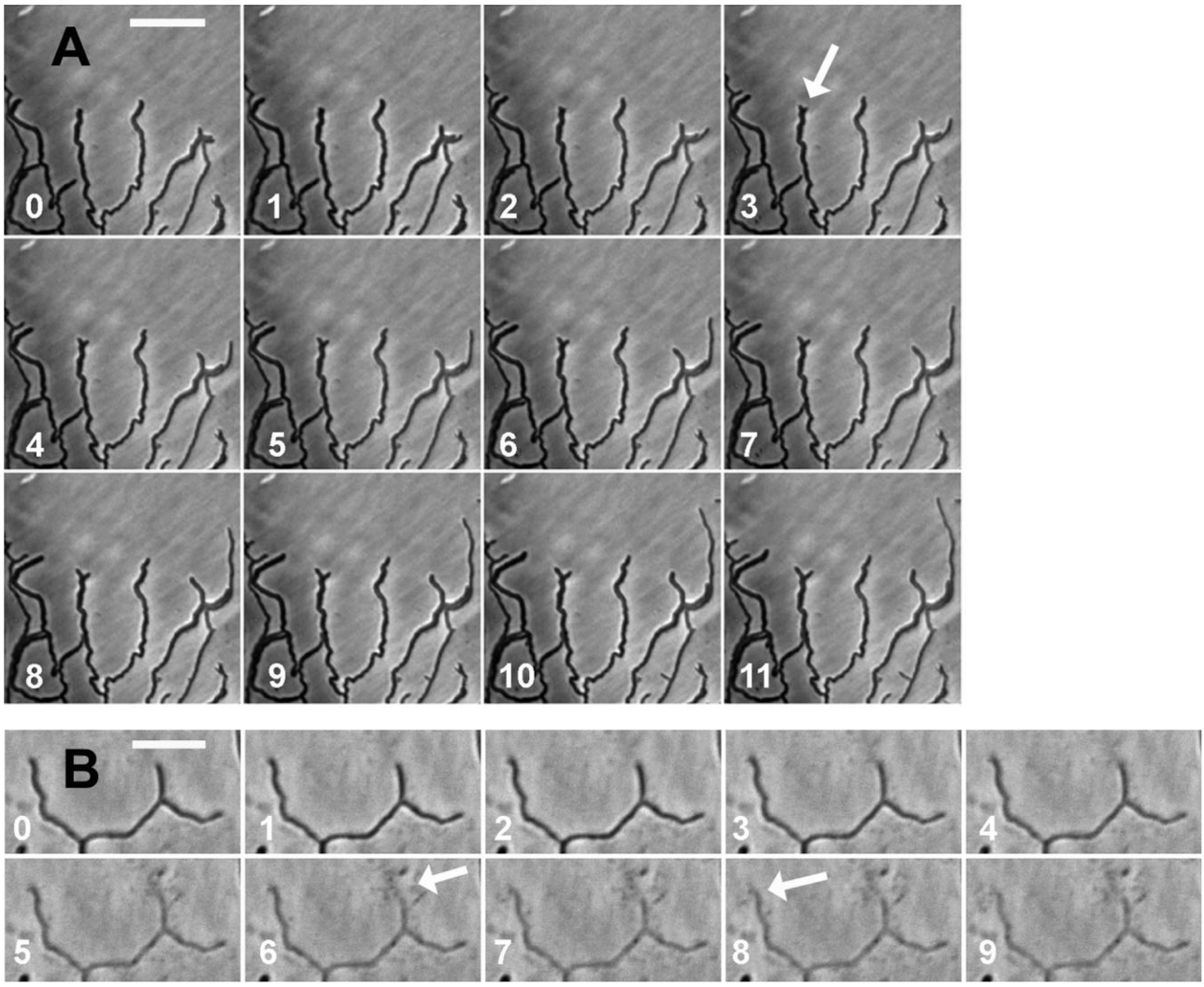

Fig. 5.

Overexpression of *clsA* weakens hyphal tips. Time-lapse microscopy, at 1 min intervals (bottom left corner of frames), of RJ110 grown with 100 μM thiostrepton showing splitting of hyphal tips (A, white arrow) and bursting of hyphal tips (B, white arrows), Horizontal white bars represent 10 μm.

Europe PMC Funders Author Manuscripts

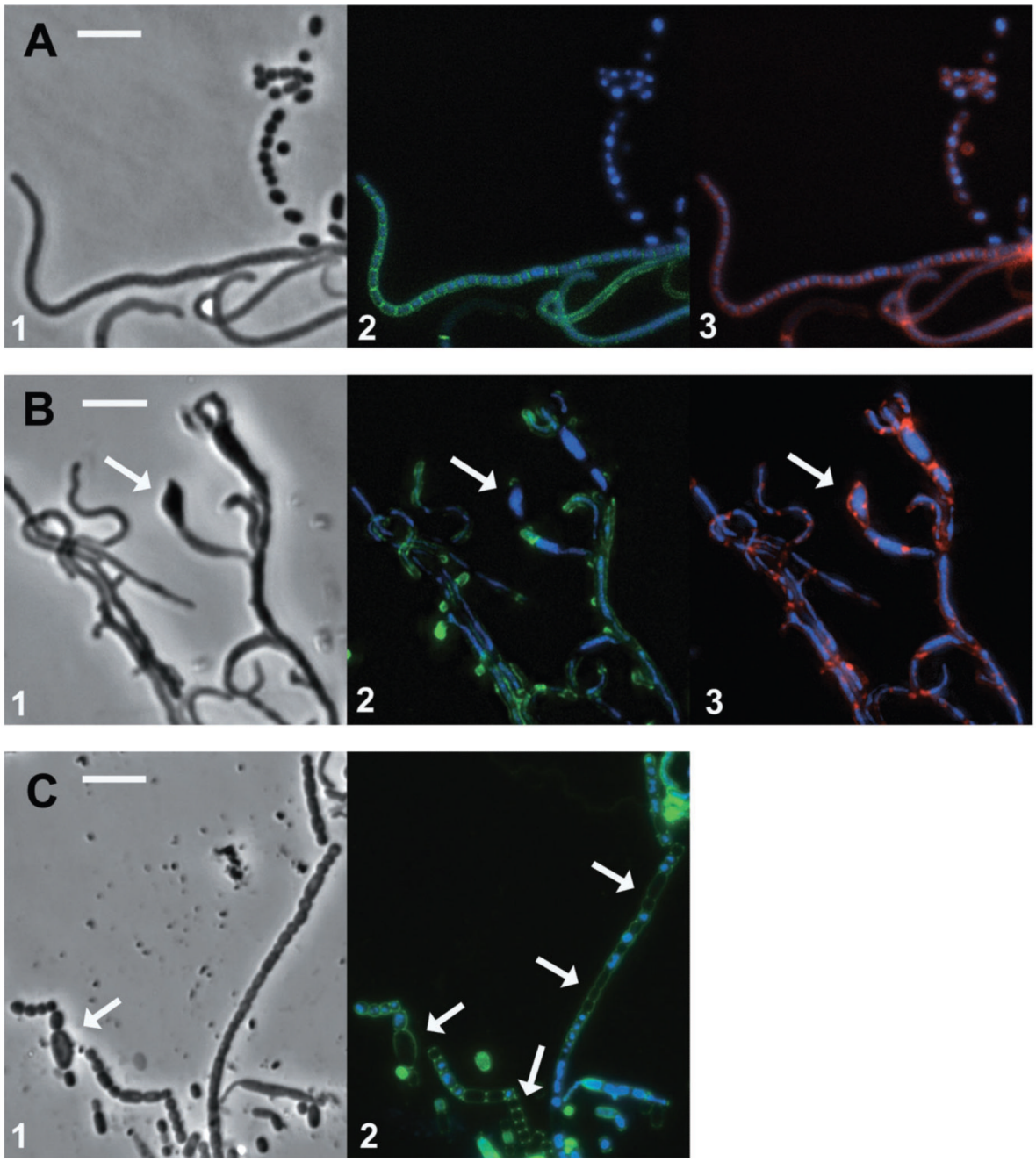

Fig. 6.

Overexpression of *clsA* causes aberrant aerial hyphae and large anucleate spores. Cultures were grown on coverslips embedded in 3MA supplemented with 100 μM thiostrepton, stained with fluorescent dyes and visualized by phase-contrast and fluorescence microscopy (see *Experimental procedures*).

A. VJ8600 aerial hyphae and spores stained with Syto42 (blue), Vancomycin-FL (green) and FM4-64 (red).

B. RJ110 aerial hyphae stained with Syto42 (blue), Vancomycin-FL (green) and FM4-64 (red). The white arrow denotes a large aberrant hypha.

C. RJ110 spores stained with Propidium Iodide (false coloured blue) and FITC-WGA (green). White arrows denote large anucleate spores. Horizontal white bars represent 5 μm.

Europe PMC Funders Author Manuscripts

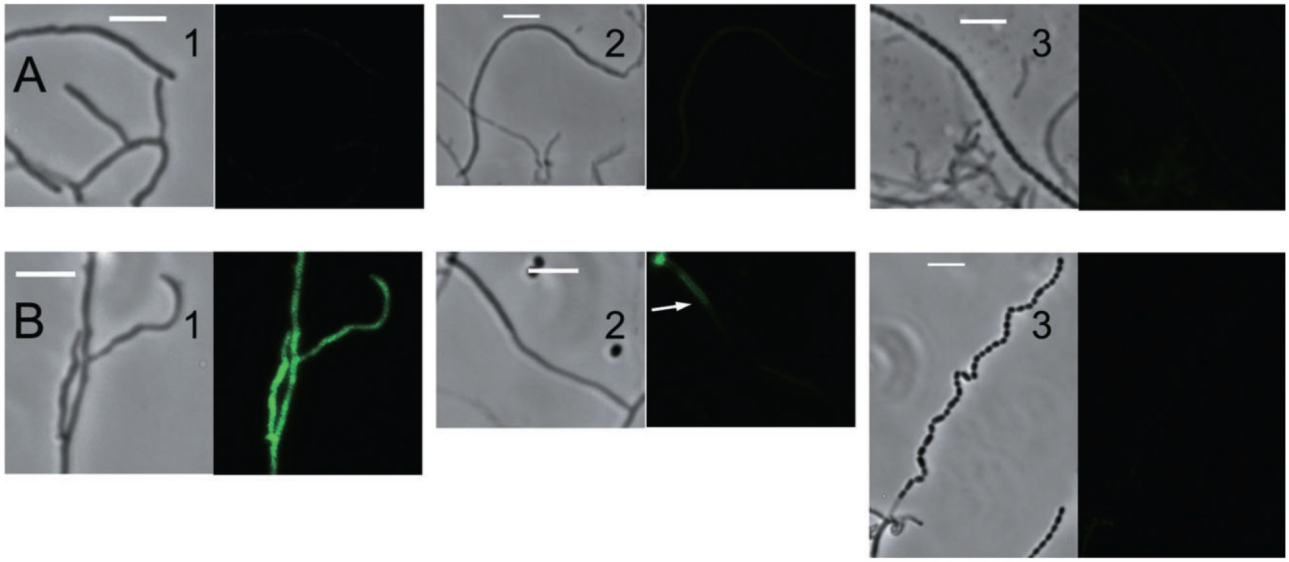

Fig. 7.

ClsA is mainly expressed in substrate hyphae and does not localize to specific sites. M145 (A) and RJ113 (B) were grown on coverslips embedded in 3MA and ClsA-EGFP visualized by phase-contrast and fluorescence microscopy. Substrate hyphae (1), aerial hyphae (2) and spore chains (3). The white arrow indicates ClsA-EGFP located at the base of an aerial hypha. Horizontal white bars represent 5 μm.

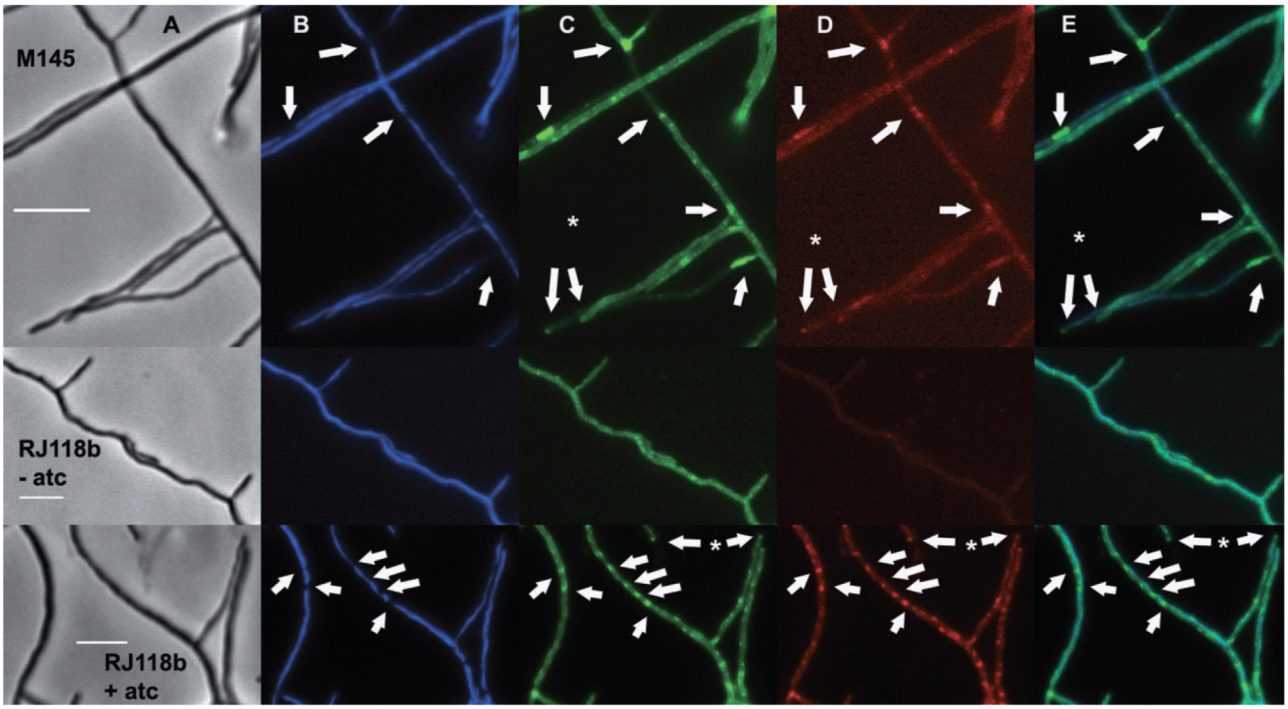

Fig. 8.

CL-rich domains localize to hyphal tips and branch points. M145 and RJ118b were grown with and without atc on coverslips embedded in 3MA, stained with Syto42 (nucleoids, B) and NAO (anionic PLs, C; CL, D) and visualized by phase-contrast (A) and fluorescence microscopy. Composite images (E) of nucleoids and anionic PL staining are also displayed. White arrows display regions of nucleic acid depletion and PL enrichment at branch points and tips (*). Horizontal white bars represent 5 μm.

Table 1

Bacterial strains and plasmids used in this study.

Plasmid or strain	Characteristics	Reference or source
pALTER 1	*E. coli* cloning vector; *tet*^{r}	Promega
pEGFP-N1	*E. coli* vector containing *egfp*; *kan*^{r}	Clontech
pMS82	Integrative vector for *Streptomyces*; *oriT*$_{RK2}$ *int attP*$_{\Phi BT1}$; *hyg*^{r}	Gregory *et al.* (2003)
pIJ8600	Integrative vector for *Streptomyces*; *oriT*$_{RK2}$ *int attP*$_{\Phi C31}$; *amf*, *ts*^{r}	Sun *et al.* (1999)
SC1A8A	Cosmid containing *clsA*; *ap*^{r}, *km*^{r}	Redenbach *et al.* (1996)
SC1A8A.2.B10	SC1A8A::Tn*5062* (in *clsA*; genome position, 1468170); *ap*^{r}, *km*^{r}, *am*^{r}	Bishop *et al.* (2004)
SC1A8A.2.E05	SC1A8A::Tn*5062* (in *rrnC*; genome position, 1468850); *ap*^{r}, *km*^{r}, *am*^{r}	Bishop *et al.* (2004)
SC1A8AΔ*cls*A	SC1A8A; *clsA* replaced with *am*^{r}; *ap*^{r}, *km*^{r}, *am*^{r}	This work
pCLS102	*clsA* cloned into pALTER1; *am*^{r}, *tet*^{r}	This work
pCLS105	*clsA* cloned into pMS82; *hyg*^{r}	This work
pCLS107	*clsA* cloned into pEGFP-N1; *km*^{r}	This work
pCLS108B	*clsA*-*egfp* in pMS82; *hyg*^{r}	This work
pCLS113A	*clsA* in pIJ8600; *am*^{r}, *tsr*^{r}	This work
pAV11B	pMS82 containing tetracycline-inducible *tcp830* promoter and *tetris*; *hyg*^{r}	Khaleel *et al.* (2011)
pAV117B1	*clsA* in pAV11b; *hyg*^{r}	This work
E. coli JM109	General cloning host	
E. coli ET12567 (pUZ8002)	Host for mobilization of DNA to *Streptomyces* by intergeneric conjugation; *tet*^{r}, *cm*^{r}, *km*^{r}	Kieser *et al.* (2000)
S. coelicolor M145	Wild type, SCP1$^-$ SCP2$^-$ Pgl$^+$	Kieser *et al.* (2000)
S. coelicolor VJ8600	M145::pIJ8600; *am*^{r}, *ts*^{r}	Sun *et al.* (1999)
S. coelicolor RJ110	M145::pCLS113A; *am*^{r}, *tsr*^{r}	This work
S. coelicolor RJ111	M145:: SC1A8AΔ *clsA*; *am*^{r}, *km*^{r} (sxo)	This work
S. coelicolor RJ113	M145Δ *clsA*::pCLS108B; *am*^{r}, *hyg*^{r}	This work
S. coelicolor RJ114	M145Δ *clsA*::pCLS105; *am*^{r}, *hyg*^{r}	This work
S. coelicolor RJ117	M145::pAV11b; *hyg*^{r}	This work
S. coelicolor RJ118a	M145::SC1A8AΔ *clsA*::pAV117B1; *am*^{r}, *km*^{r}, *hyg*^{r} (sxo)	This work
S. coelicolor RJ118b	M145Δ *clsA*::pAV117B1; *am*^{r}, *hyg*^{r} (dxo)	This work

sxo, single cross-over; dxo, double cross-over.